

# Increase of Voltage-Sensitive Calcium Channels and Calcium Accumulation in Skeletal Muscles of Streptozocin-Induced Diabetic Rats

Tsutomu Ogawa, Atsunori Kashiwagi, Ryuichi Kikkawa, and Yukio Shigeta

The number of voltage-sensitive calcium channels (VOCC) in triceps surae muscle membrane fractions isolated from control and streptozocin (STZ)-induced diabetic rats was determined using [ $^3\text{H}$ ]PN200-110, a dihydropyridine derivative, as a ligand. Furthermore, quantitative analysis of calcium in soleus muscle fibers was performed by the calcium oxalate-pyroantimonate method and x-ray microanalysis. The maximum binding ( $B_{\text{max}}$ ) of [ $^3\text{H}$ ]PN200-110 in skeletal muscle membrane isolated from 10-week diabetic rats ( $1,091 \pm 77$  fmol/mg protein) was increased significantly by 91% as compared with the control value ( $572 \pm 32$  fmol/mg protein), without a significant change in  $K_d$ . The increase in  $B_{\text{max}}$  of [ $^3\text{H}$ ]PN200-110 was dependent on the duration of diabetes, and was not found until 6 weeks after STZ injection. Insulin treatment for 8 weeks after induction of diabetes normalized  $B_{\text{max}}$  to the control level ( $583 \pm 53$  fmol/mg protein). Precipitates of calcium antimonate, identified by x-ray microanalysis, were observed much more frequently in specimens from 10-week diabetic rats versus controls. The increase in the incidence of precipitates was not observed in 3-week diabetic rats and was suppressed by 8 weeks' insulin treatment. These results indicate that the number of VOCC in chronically diabetic rats was increased in the sarcolemmal membrane of skeletal muscle and that calcium was accumulated inside skeletal muscle fibers.

Copyright © 1995 by W.B. Saunders Company

**A**BNORMALITIES of muscle strength were reported in skeletal muscles of diabetic rats.<sup>1,2</sup> To explain the hyperfunction of skeletal muscles during the development of diabetes, the handling of intracellular  $\text{Ca}^{2+}$  by subcellular structures has been studied. An increase in sarcoplasmic reticular  $\text{Ca}^{2+}$  pump activity<sup>2</sup> and an increase in the contractile protein  $\text{Ca}^{2+}$ -related adenosine triphosphatase (ATPase) activity<sup>3</sup> may be associated with the hyperfunction of diabetic skeletal muscles.

Recently, we have shown the increase in voltage-sensitive calcium channels (VOCC) on cardiac sarcolemma of diabetic rats.<sup>4</sup> Furthermore, the increase in VOCC on hind leg skeletal muscles has also been shown.<sup>5</sup> The increase in VOCC suggests that  $\text{Ca}^{2+}$  influx into skeletal muscle fibers through sarcolemmal membrane in diabetic rats is increased, and therefore  $\text{Ca}^{2+}$  can be accumulated in skeletal muscles of diabetic animals. Calcium accumulation may be related to the hyperfunction of diabetic skeletal muscles.

To further evaluate abnormalities of VOCC in skeletal muscles, such as the effect of duration of diabetes, the reversibility of abnormalities by insulin treatment, and the difference in those abnormalities between slow- and fast-twitch muscle fibers, we performed binding studies on VOCC in skeletal muscle membranes of diabetic rats. Furthermore, to prove the hypothesis that diabetes mellitus induces intracellular  $\text{Ca}^{2+}$  accumulation in skeletal muscles, we evaluated calcium content in skeletal muscle cells using the oxalate-pyroantimonate method and x-ray microanalysis.

## MATERIALS AND METHODS

### Animals

Male Sprague-Dawley rats weighing 150 to 200 g were divided into two groups. Diabetes was induced in one group of rats by injection of streptozocin ([STZ] 55 mg/kg body weight intravenously). The other group of rats received an injection of citrate-buffered vehicle only. A subgroup of diabetic rats were treated by insulin injection (porcine ultralente insulin 8 U/d subcutaneously) for 8 weeks from 2 weeks after STZ injection. All animals were maintained on standard animal chow and water ad libitum. Rats were used in the experiment 3, 6, 10, and 12 weeks after induction

of diabetes. Animals were killed under diethylether anesthesia after blood samples were obtained from the inferior vena cava. Plasma glucose and insulin levels were measured by the hexokinase method<sup>6</sup> and radioimmunoassay,<sup>7</sup> respectively. Characteristics of the experimental animals are shown in Table 1.

### Preparation of Triceps Surae Muscle Membrane

Crude plasma membrane fractions were prepared by the previously described method with some modifications.<sup>8</sup> Briefly, rats were killed and the triceps surae muscle was quickly removed, minced, and homogenized in 6 vol cold 50-mmol/L Tris hydrochloride buffer (pH 7.4) containing 5 mmol/L EDTA, 0.3 mmol/L phenylmethylsulfonyl fluoride (PMSF), 50 U/mL aprotinin, and 10  $\mu\text{mol/L}$  benzetonium chloride. Homogenates were centrifuged at  $500 \times g$  for 10 minutes, and supernatants were centrifuged at  $40,000 \times g$  for 15 minutes. The pellets were suspended and homogenized in 10 mmol/L histidine buffer (pH 7.5) containing 0.75 mol/L NaCl to extract contractile protein. Aliquots were then centrifuged at  $105,000 \times g$  for 30 minutes. The resultant precipitates were washed with 50 mmol/L Tris hydrochloride buffer (pH 7.5) containing 0.1 mmol/L PMSF and were used as crude skeletal muscle membrane fractions.

Protein concentration was measured as described by Lowry et al<sup>9</sup> with bovine serum albumin as a standard. 5'-Nucleotidase activity was measured according to the method described by Newby et al.<sup>10</sup> Recovery of protein in membrane fractions isolated from control, diabetic, and insulin-treated diabetic rats was  $2.5\% \pm 0.2\%$ ,  $2.7\% \pm 0.3\%$ , and  $2.7\% \pm 0.3\%$ , respectively (mean  $\pm$  SE).

### Calcium Channel Binding Assay

The number of dihydropyridine-sensitive  $\text{Ca}^{2+}$  channels in membrane fractions was measured according to a previously described method with some modifications.<sup>11</sup> Briefly, 50  $\mu\text{g}$  membrane protein was incubated at  $37^\circ\text{C}$  for 15 minutes under 1 mL

---

From the Third Department of Internal Medicine, Shiga University of Medical Science, Shiga, Japan.

Submitted October 27, 1994; accepted February 7, 1995.

Address reprint requests to Atsunori Kashiwagi, MD, Third Department of Internal Medicine, Shiga University of Medical Science, Tukinowa-cho, Seta, Ohtsu, Shiga, Japan 520-21.

Copyright © 1995 by W.B. Saunders Company  
0026-0495/95/4411-0015\$03.00/0

**Table 1. Characteristics of Control, Untreated Diabetic, and Insulin-Treated Diabetic Rats**

Group	No. of Rats	Body Weight (g)	Wet Weight of Triceps Surae Muscle (g)	Plasma Glucose (mmol/L)	Plasma Insulin ( $\mu$ U/mL)
3-week					
Control	4	350 $\pm$ 7	4.39 $\pm$ 0.15	7.3 $\pm$ 0.4	23.2 $\pm$ 0.8
Diabetic	4	229 $\pm$ 17†	2.57 $\pm$ 0.11†	28.6 $\pm$ 1.8†	6.3 $\pm$ 1.4†
6-week					
Control	4	384 $\pm$ 6	5.20 $\pm$ 0.30	7.3 $\pm$ 0.3	17.3 $\pm$ 1.8
Diabetic	4	237 $\pm$ 5†	2.61 $\pm$ 0.32†	28.0 $\pm$ 1.0†	3.0 $\pm$ 1.1†
10-week					
Control	7	463 $\pm$ 12	5.30 $\pm$ 0.33	6.4 $\pm$ 0.3	22.5 $\pm$ 2.6
Diabetic	8	234 $\pm$ 13†	2.99 $\pm$ 0.19†	26.6 $\pm$ 0.6†	4.7 $\pm$ 0.3*
Treated	7	403 $\pm$ 18§	4.50 $\pm$ 0.32§	5.7 $\pm$ 0.4§	54.8 $\pm$ 10.2‡
12-week					
Control	7	493 $\pm$ 13	5.79 $\pm$ 0.12	7.2 $\pm$ 0.3	24.0 $\pm$ 4.9
Diabetic	7	292 $\pm$ 15†	2.90 $\pm$ 0.15†	26.8 $\pm$ 1.1†	5.8 $\pm$ 1.4*

NOTE. Values are expressed as the mean  $\pm$  SE.\* $P < .05$ , † $P < .01$ : v control rats.‡ $P < .05$ , § $P < .01$ : v diabetic rats.

||Diabetic rats with insulin treatment for 8 weeks.

50-mmol/L Tris hydrochloride (pH 7.5) and 0.1 mmol/L PMSF containing 100 to 2,500 pmol/L [ $^3$ H]PN200-110 (isopropyl 4-(4-benzofurazanyl)-1,4-dihydro-2,6-dimethyl-5-methoxycarbonyl-pyridine-3-carboxylate). The incubation was terminated by addition of 4 mL cold 10-mmol/L Tris hydrochloride (pH 7.4) buffer and kept at 4°C for 30 minutes. Membrane-bound [ $^3$ H]PN200-110 was

separated from free [ $^3$ H]PN200-110 by vacuum filtration through Whatman GF/B glass fiber filters (Clifton, NJ). Nonspecific binding was determined under 10  $\mu$ mol/L nitrendipine (<35% of the total binding in the highest ligand concentration). Maximum binding ( $B_{\max}$ ) and  $K_d$  for [ $^3$ H]PN200-110 were calculated from Scatchard analysis with linear regression.

#### Fixation With Microwave Irradiation

Fixation of soleus muscle was performed as described previously with some modifications<sup>12,13</sup> using the microwave irradiation method.<sup>14</sup> Soleus muscles were removed from pentobarbital-anesthetized (1 mg/10 g body weight subcutaneously) rats and immediately cut into small pieces ( $\sim 0.8$  cm<sup>3</sup>) in the fixative, a mixed aldehyde solution consisting of 2% paraformaldehyde and 0.5% glutaraldehyde, 60 mmol/L potassium oxalate, and 0.1% tannic acid in 0.1 mol/L sodium cacodylate buffer adjusted to pH 7.2 with KOH. Tissue blocks in the fixing solution were subjected to microwave irradiation at room temperature for 20 seconds using a household microwave oven (2.45 GHz, 500W). The temperature of the fixing solution was less than 35°C on termination of microwave irradiation. Tissue blocks were cut into small pieces, 1 to 3 mm<sup>3</sup>, in the fixative. The samples were kept immersed in the fixative for an additional 60 minutes and then rinsed in 60 mmol/L potassium oxalate in 2% sucrose at pH 7.4, and were postfixed with 1% osmium tetroxide and 2% potassium pyroantimonate for 2 hours at room temperature. The tissues were rinsed in water adjusted to pH 10 with KOH for 15 minutes to wash out unreacted potassium pyroantimonate. Subsequently, the tissues were dehydrated through an ascending series of ethanols and embedded in Epon. Seventy-

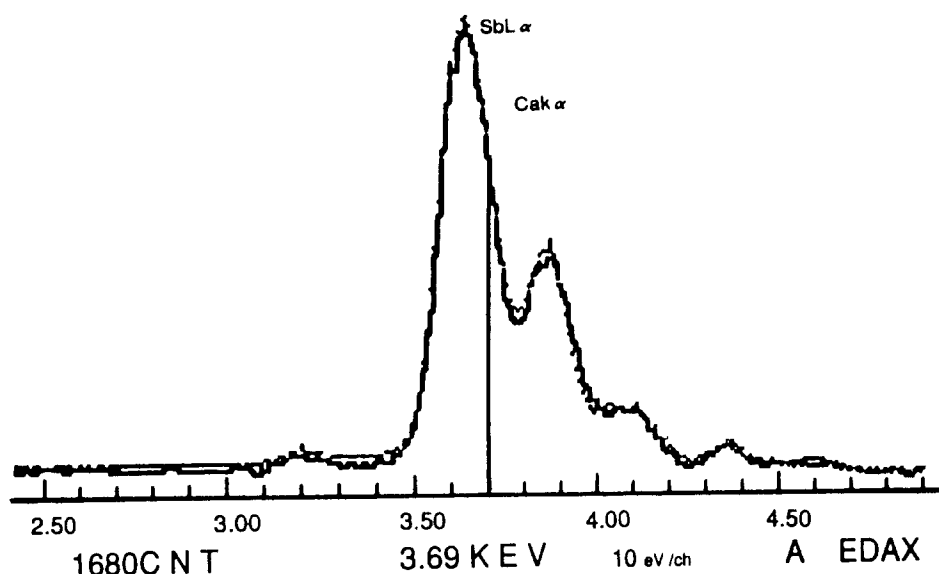


Fig 1. Energy spectrum by x-ray microanalysis for precipitates of calcium antimonate in a sample specimen. Results of analysis by EDAX PV9800 system are shown below. Horizontal line: energy level; total count was 1,680 for 200 seconds. Vertical line at 3.69 KeV: K $\alpha$  calcium peak. SB L, antimonate L peak; CA K, calcium K peak. CPS (counts per second) shows x-ray intensity of SB L and CA K isolated from spectrum. WT% ELEM and AT% ELEM, weight ratio and volume ratio of Sb to Ca calculated by PV9800.

ELEM	CPS	WT%	AT%
		ELEM	ELEM
SB L	110.3	85.6	66.1
CA K	51.5	14.4	33.9
		-----	-----
		100.0	100.0

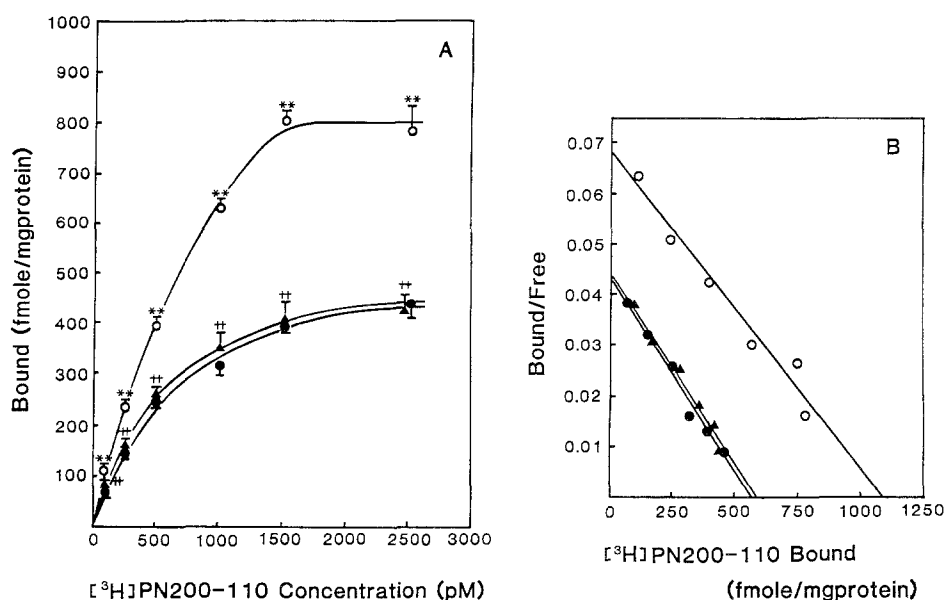


Fig 2. (A) Specific  $[^3\text{H}]\text{PN200-110}$  binding to membrane fractions of triceps surae muscle isolated from control (●), 10-week untreated diabetic (○), and 10-week insulin-treated diabetic (▲) rats. Mean  $\pm$  SE ( $n = 4$ ). \*\* $P < .01$  v control; \*\* $P < .01$  v untreated diabetic. (B) Mean Scatchard plots of  $[^3\text{H}]\text{PN200-110}$  binding to membrane fractions of triceps surae muscle.

nanometer sections were picked up on nickel grids, stained with uranyl acetate and lead citrate, and examined with a JEOL 1200EX electron microscope (Japan Electron Optical Laboratory, Tokyo, Japan).

#### X-ray Microanalysis for Calcium Detection and Relative Quantification of Calcium

X-ray microanalysis was performed with a JEOL 1200EX electron microscope equipped with an EDAX PV9800 energy-dispersive spectrometer (Philips Electronic Instruments, Mahwah, NJ) on unstained 100-nm sections on nylon grids. Precipitates of calcium antimonate ( $\text{Ca}[\text{Sb}(\text{OH})_6]_2$ ) were made in vitro and set on a nylon grid as a sample specimen. X-ray microanalysis was performed for these precipitates with a PV9800 system. Results of the analysis are shown in Fig 1.  $K\alpha$  and  $K\beta$  calcium peaks ( $K\alpha$ , 3.690 keV;  $K\beta$ , 4.012 keV) and  $L\alpha$  and  $L\beta$  antimonate peaks ( $L\alpha$ , 3.604 keV;  $L\beta_1$ , 3.843 keV;  $L\beta_2$ , 4.100 keV) were so close that the energy spectrum shown in Fig 1 is the summation of energy spectra from the calcium K peak and antimonate L peak. The PV9800 system could clearly divide the characteristic x-ray intensity of Ca from that of Sb, judging from the weight ratio and volume ratio of Ca to Sb (ideal weight ratio of Ca to Sb, 14.1:85.9; ideal volume ratio of Ca to Sb, 33.3:66.7).

Quantities of calcium antimonate precipitates were evaluated by observation of specimens. Furthermore, x-ray microanalysis was performed on a  $200 \times 200$ -nm area in mitochondria. Accelerating voltage was 60 kV, and collection time of spectral lines was 200

seconds. The intensity of characteristic x-rays of Ca was compared between specimens from control and diabetic rats.

#### Chemicals

$[^3\text{H}]\text{PN200-110}$  (2,597.4 GBq/mmol) and  $[^{14}\text{C}]\text{adenosine monophosphate}$  were purchased from New England Nuclear (Boston, MA), nitrendipine was a gift from Yoshitomi Pharmaceutical (Osaka, Japan), and STZ was generously provided by Upjohn (Kalamazoo, MI). All other chemicals were reagent-grade products obtained from commercial sources.

#### Statistical Analysis

Data are expressed as the mean  $\pm$  SE. Statistical significance of differences in mean values for intensity of characteristic x-ray from mitochondria between control and diabetic rats was determined by Wilcoxon's test. For all other data, statistical significance was determined by ANOVA.  $P$  less than .05 was considered significant.

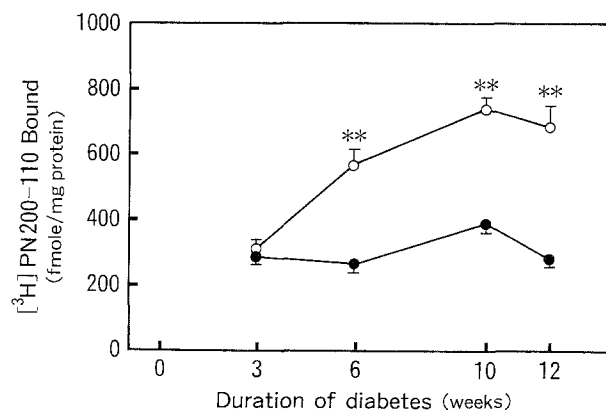


Fig 3. Effect of duration of diabetes on specific  $[^3\text{H}]\text{PN200-110}$  binding to membrane fractions of triceps surae muscle isolated from control (●) and 10-week diabetic (○) rats (concentration of the ligand, 2,000 pmol/L). Mean  $\pm$  SE ( $n = 4$ ). \*\* $P < .01$  v control.

Table 2. Characteristics of  $[^3\text{H}]\text{PN200-110}$  Binding to Membrane Fractions Isolated From Control, Untreated Diabetic, and Insulin-Treated Diabetic Rats

Group	No. of Rats	5'-Nucleotidase (nmol/min/mg protein)	$[^3\text{H}]\text{PN200-110}$	
			Binding Sites (fmol/mg protein)	$K_d$ (pmol/L)
Control	4	$16.0 \pm 1.3$	$572 \pm 32$	$659 \pm 49$
Diabetic	4	$15.9 \pm 1.5$	$1,091 \pm 77^\dagger$	$794 \pm 35$
Treated*	4	$19.9 \pm 3.4$	$583 \pm 53$	$697 \pm 54$

NOTE. Values are expressed as the mean  $\pm$  SE.

\*Diabetic rats with insulin treatment for 8 weeks.

$^\dagger P < .01$  v control and v insulin-treated diabetic rats.

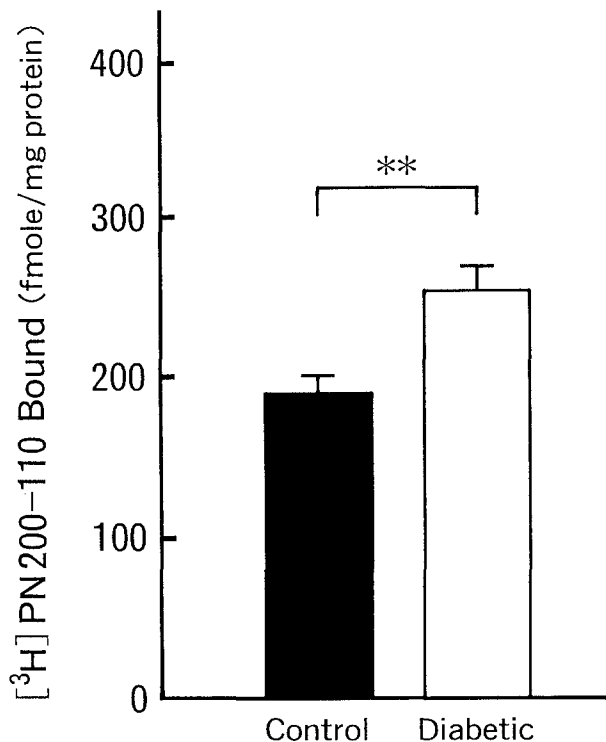


Fig 4. Specific [<sup>3</sup>H]PN200-110 binding to membrane fractions of soleus muscle isolated from control and 10-week diabetic rats. Mean ± SE (n = 4). \*\**P* < .01 v control.

## RESULTS

### Body Weight, Triceps Surae Muscle Weight, and Serum Glucose and Insulin Levels

All diabetic rats showed significantly higher plasma glucose concentrations (*P* < .01) as compared with controls. Furthermore, both body weight and triceps surae muscle weight were less (*P* < .05) in diabetic rats than in control animals. Insulin-treated diabetic rats showed significant improvement of both body weight and triceps surae muscle weight versus 10-week diabetic rats (Table 1).

### [<sup>3</sup>H]PN200-110 Binding to Membrane Fraction of Triceps Surae Muscle

[<sup>3</sup>H]PN200-110 binding to triceps surae muscle membrane from 10-week diabetic rats was significantly increased (*P* < .01) at all concentrations versus 10-week control rats (Fig 2A). The increase in [<sup>3</sup>H]PN200-110 binding in diabetic rats was completely normalized to control levels by insulin treatment for 8 weeks. Figure 2B shows linear Scatchard plots of [<sup>3</sup>H]PN200-110 binding. The *B*<sub>max</sub> of the diabetic group was 91% higher than that of the control group. The increase in *B*<sub>max</sub> in the diabetic group was completely normalized by insulin treatment for 8 weeks (Table 2).

The increase in [<sup>3</sup>H]PN200-110 binding to membrane fraction of triceps surae muscle was dependent on the duration of diabetes (Fig 3). The binding in 3-week diabetic rats (305 ± 22 fmol/mg protein) was similar to that in controls (295 ± 14 fmol/mg protein) at a [<sup>3</sup>H]PN200-110

concentration of 2,000 pmol/L. However, binding was significantly (*P* < .01) increased in 6-week diabetic rats (563 ± 14 fmol/mg protein) as compared with controls (266 ± 25 fmol/mg protein). The increase in [<sup>3</sup>H]PN200-110 binding was maintained until 12 weeks after induction of diabetes.

### [<sup>3</sup>H]PN200-110 Binding to Membrane Fraction of Soleus Muscle

[<sup>3</sup>H]PN200-110 binding to membrane fraction isolated from soleus muscle composed almost entirely of slow-twitch fibers was also significantly (*P* < .01) increased in 10-week diabetic rats (254 ± 16 fmol/mg protein) as compared with controls (191 ± 22 fmol/mg protein) at a [<sup>3</sup>H]PN200-110 concentration of 2,000 pmol/L (Fig 4).

### Identification of Calcium in Electron-Dense Deposits in Soleus Muscle Cells

A typical soleus muscle specimen from a control rat is shown in Fig 5A. Fine precipitates were mainly observed in mitochondria, sarcoplasmic reticulum, and nucleus (the

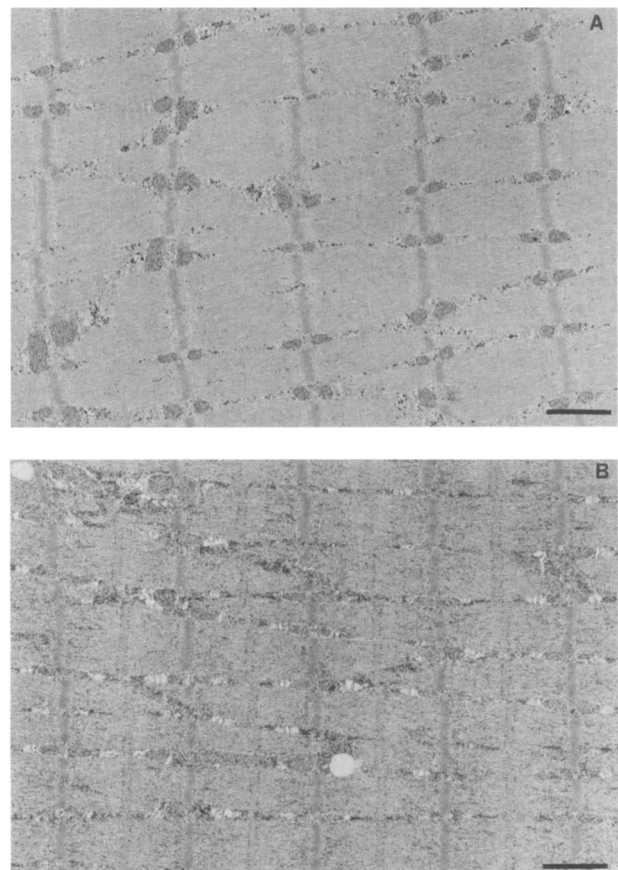


Fig 5. (A) Specimen of soleus muscle from control rat. Fine dense precipitate was observed in mitochondria and sarcoplasmic reticulum, and some was seen among myofibrils. (B) Specimen of soleus muscle from 10-week diabetic rat. Fine dense precipitate was also observed. The distribution pattern was similar to that of controls, but the amount of precipitate was much greater in the specimen from diabetic rat. Lipid droplets were observed. Bar = 1 μm.

nucleus is not shown in the figure). X-ray microanalysis was performed on the area selected in the intercellular space that was observed to contain aggregated precipitate. The intercellular space was selected because it had the lowest background. The energy spectrum obtained and the intensity of characteristic x-rays of calcium are shown in Fig 6. Results of analysis using the EDAX PV9800 system showed that precipitates observed in the specimen were calcium antimonate, judging from the weight and volume ratios of calcium to antimonate.

#### *Precipitates of Calcium Antimonate in Soleus Muscle Cells*

A typical specimen of soleus muscle from a 10-week diabetic rat is shown in Fig 5B. Fine precipitates were mainly observed in mitochondria, sarcoplasmic reticulum, and nucleus, as observed in control specimens, and also among myofibrils, especially near Z bands. However, precipitates in the diabetic specimen were observed in much greater amounts than in controls.

Ultrastructural examination of soleus muscle specimens from 3-week diabetic rats (not shown) showed no increase in the amount of calcium antimonate precipitate, and no difference in its distribution was observed as compared with controls (not shown).

Ultrastructural examination of specimens from soleus

muscles of 10-week diabetic rats with insulin treatment for 8 weeks showed no difference as compared with those of control rats (Fig 7), indicating normalization of calcium deposition in muscle cells.

#### *Relative Quantification of Calcium*

Figure 8 shows histograms of intensity of characteristic x-rays of calcium analyzed with the EDAX PV9800 system. X-ray microanalysis was performed on an area of  $200 \times 200$  nm set on the mitochondria. The mean value for the intensity of characteristic x-ray of calcium from soleus muscles of diabetic rats was significantly higher than that of controls ( $P < .01$ ). The distribution of x-ray count was broader in specimens from diabetic rats versus controls. Furthermore, four columns were observed in the high-count area separated from the other columns in specimens from diabetic animals.

#### DISCUSSION

The  $B_{\max}$  of [ $^3\text{H}$ ]PN200-110 binding to the membrane fraction of triceps surae muscle isolated from 10-week diabetic rats was 91% higher than that isolated from controls, with no significant difference in  $K_d$ . The increase in  $B_{\max}$  supports the results described previously in hind leg

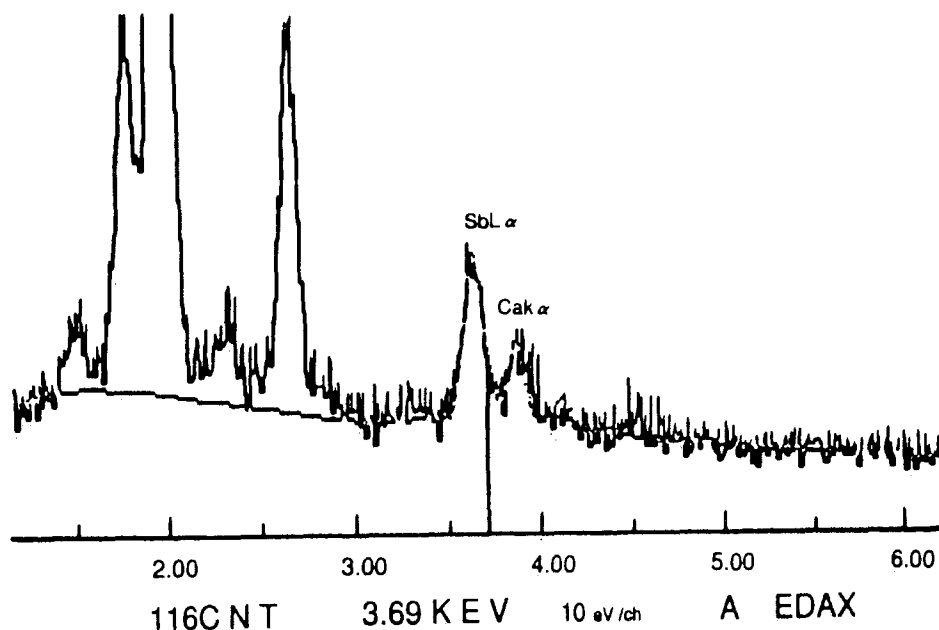


Fig 6. Energy spectrum by x-ray microanalysis of precipitates in specimens from soleus muscle of control rats. Results of analysis by EDAX PV9800 system are shown below. Horizontal line: energy level; total count was 116 for 200 seconds. Vertical line at 3.69 KeV:  $K\alpha$  calcium peak. SB L, antimonate L peak; CA K, calcium K peak. CPS (counts per second) shows x-ray intensity of SB L and CA K isolated from the spectrum. WT% ELEM and AT% ELEM, weight ratio and volume ratio of Sb to Ca calculated by PV9800.

		WT%	AT%
ELEM	CPS	ELEM	ELEM
SB L	4.7	85.2	65.5
CA K	2.3	14.8	34.5
		-----	-----
		100.0	100.0

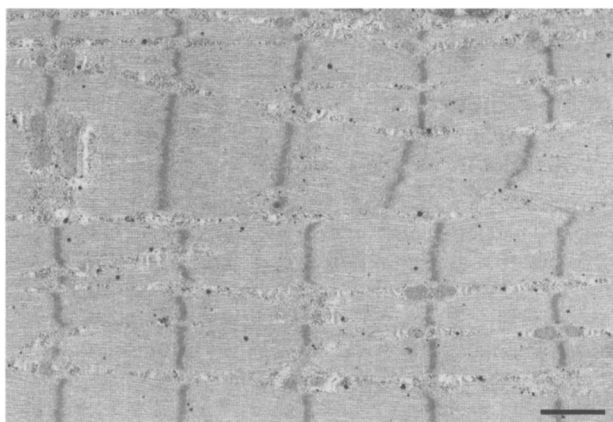


Fig 7. Specimen of soleus muscle from 10-week diabetic rat following insulin treatment for 8 weeks. The amount of fine dense precipitate was normalized. Bar = 1  $\mu$ m.

skeletal muscles of STZ-induced diabetic rats.<sup>5</sup> [<sup>3</sup>H]PN200-110, a dihydropyridine derivative, labels the  $\alpha_1$ -subunit of L-type  $\text{Ca}^{2+}$  channels.<sup>15</sup> The increase in [<sup>3</sup>H]PN200-110 binding to the membrane fraction shows an increase in VOCC on triceps surae muscle membrane. Membrane purification was performed with the same amounts of triceps surae muscle, and no significant difference was observed in recovery of either protein (above-mentioned) or 5'-nucleotidase activity (Table 2). Thus, the difference in [<sup>3</sup>H]PN200-110 binding among the three groups was not derived from the difference in the purification process.

[<sup>3</sup>H]PN200-110 binding to the membrane fraction isolated from soleus muscles of 10-week diabetic rats was increased by 33% versus controls. The soleus muscle is almost entirely composed of slow-twitch muscle fibers, although the gastrocnemius muscle, which is the main component of the triceps surae muscle, has more fast-twitch muscle fibers. Therefore, the increase in VOCC may occur generally in diabetic skeletal muscles, and the increase may be more marked in fast-twitch than in slow-twitch muscle fibers. VOCC concentration in 3-week diabetic rats was similar to that in controls, ruling out the possibility of toxicity of STZ. The increase in VOCC was observed in the 6-week diabetic group and continued until 12 weeks. Glycemic control by insulin injection completely reversed the increase in VOCC.

Much greater amounts of precipitate were observed in specimens from skeletal muscle of 10-week diabetic rats as compared with control rats by electron microscopic evaluation after fixation of muscle tissues by the oxalate pyroantimonate method. X-ray microanalysis using the EDAX PV9800 system confirmed that the precipitates were calcium antimonate. These results indicated that calcium content is higher in skeletal muscle fibers of 10-week diabetic rats versus controls. The results of x-ray microanalysis for mitochondria supported the increase in calcium content in mitochondria of diabetic skeletal muscles. Distribution of precipitate was both dense and homogeneous in mitochondria, making mitochondria suitable for analysis of calcium content. The mean value for the intensity of

characteristic x-ray of calcium from mitochondria in diabetic skeletal muscle was 30% higher than in control muscle. Greater than 3 weeks of the diabetic state was required for calcium accumulation, indicating that the accumulation may not be induced by acute toxicity of STZ.

Paulus and Grossie<sup>1</sup> reported that the average specific twitch force in diabetic soleus muscles was greater than in controls after 32 days of the diabetic state, but it was not different between diabetic soleus muscles and controls after 16 days of diabetes. Ganguly et al<sup>2</sup> reported that the force of isometric contraction of the hamstring muscle is significantly stronger in diabetic animals than in controls. They speculated that an increase both in the sarcoplasmic reticular  $\text{Ca}^{2+}$  pump activity<sup>2</sup> and in the contractile protein  $\text{Ca}^{2+}$ -related ATPase activity<sup>3</sup> may be associated with hyperfunction of skeletal muscles in diabetic rats. The increase in calcium content in skeletal muscle fibers shown

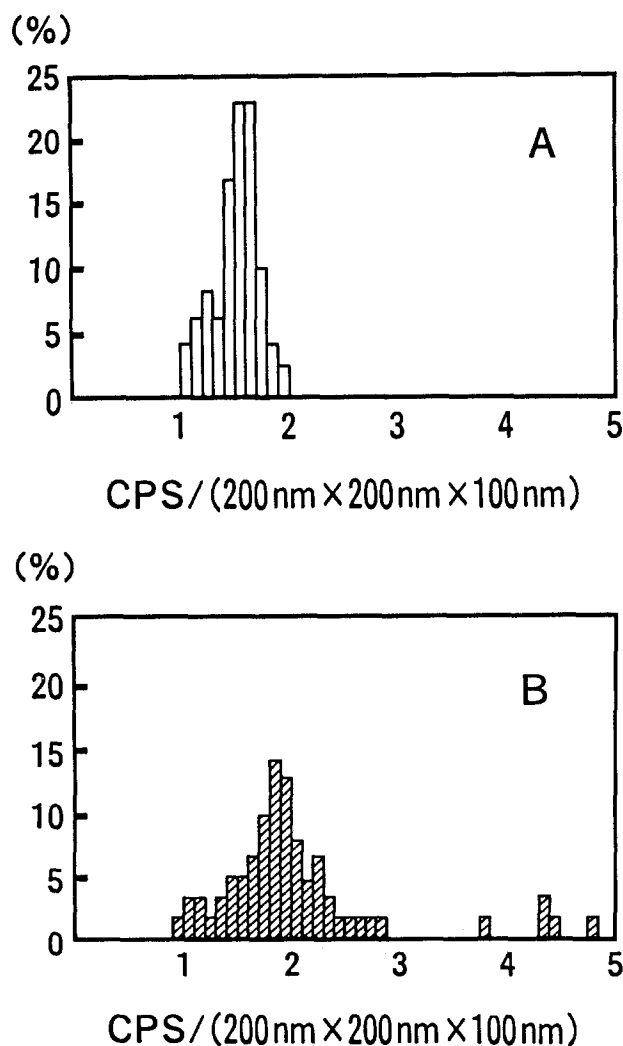


Fig 8. Histogram of intensity of characteristic x-rays of calcium with x-ray microanalysis performed on an area of 200  $\times$  200 nm set on the mitochondria. (A) Control rats, n = 50; (B) 10-week diabetic rats, n = 65.

in the present study may be one of the causes of the skeletal muscle hyperfunction. Although no direct evidence has been presented, it is possible that the hyperfunction of skeletal muscle in the diabetic state is one of the explanations for the frequent muscle cramp observed in the lower extremities of diabetic patients.

A decrease in  $\text{Na}^+\text{-K}^+\text{-ATPase}$  concentration in diabetic skeletal muscles<sup>16</sup> may be associated with an increased intracellular  $\text{Na}^+$  concentration, which may suppress  $\text{Na}^+$ -dependent  $\text{Ca}^{2+}$  uptake. In addition to these abnormal ion-transport systems in diabetes, the increase in VOCC concentration, which we determined in the present study, may also be associated with calcium overloading in diabetic skeletal muscle cells. With regard to  $\text{Ca}^{2+}$  efflux, Taira et al<sup>17</sup> reported that both sarcolemmal  $\text{Na}^+$ -dependent and ATP-dependent  $\text{Ca}^{2+}$  uptake were increased in skeletal muscle of diabetic rats, which is opposed to the result speculated from the decrease in  $\text{Na}^+\text{-K}^+\text{-ATPase}$  concentration. It is possible that the increase in sarcolemmal  $\text{Ca}^{2+}$  transport activity in diabetic skeletal muscle cells is explained by the adaptation to calcium accumulation.

From ultrastructural analysis of diabetic skeletal muscle, disappearance of mitochondrial cristae and swelling of mitochondria were reported.<sup>18</sup> Calcium accumulation may be related to these ultrastructural changes in mitochondria. When cytoplasmic calcium increases within the physiological range, calcium pumps in the inner membrane of mitochondria can regulate mitochondrial calcium concentration.<sup>19,20</sup> However, recently, cytoplasmic calcium concentrations above the physiological range were reported in some pathological conditions such as ischemia-reperfusion states and following exposure to oxidative stress. In such conditions, calcium is accumulated in mitochondria, resulting in mitochondrial injury.<sup>21,22</sup> A long duration of diabetes also induces calcium accumulation in mitochondria, suggesting a similar pathophysiological mechanism in these states.

#### ACKNOWLEDGMENT

The authors wish to thank Dr Vinci Mizuhira for discussion and advice on the histological aspect of this study, and Hiroshi Hasegawa and Mitsuru Notoya for assistance in specimen preparation and electron microscopy.

#### REFERENCES

1. Paulus SF, Grossie J: Skeletal muscle in alloxan diabetes. *Diabetes* 32:1035-1039, 1983
2. Ganguly PK, Mathur S, Gupta MP, et al: Calcium pump activity of sarcoplasmic reticulum in diabetic rat skeletal muscle. *Am J Physiol* 251:E515-E523, 1986
3. Ganguly PK, Taira Y, Elimban V, et al: Altered contractile proteins in skeletal muscle of diabetic rats. *Am J Physiol* 253:E395-E400, 1987
4. Nishio Y, Kashiwagi A, Ogawa T, et al: Increase in [ $^3\text{H}$ ]PN200-110 binding to cardiac muscle membrane in streptozocin-induced diabetic rats. *Diabetes* 39:1064-1069, 1990
5. Lee SL, Dhalla NS:  $\text{Ca}^{2+}$ -channels and adrenoceptors in diabetic skeletal muscle. *Biochem Biophys Res Commun* 184:353-358, 1992
6. Hoffman WS: A rapid photometric method for the determination of glucose in blood and urine. *J Biol Chem* 248:12051-12055, 1973
7. Hales C, Randle P: Immunoassay of insulin with insulin antibody precipitate. *Biochem J* 88:137-146, 1963
8. Jones JR, Besch HR Jr, Fleming JW, et al: Separation of vesicles of cardiac sarcolemma from vesicles of cardiac sarcoplasmic reticulum. *J Biol Chem* 254:530-539, 1979
9. Lowry OH, Rosebrough HJ, Farr AL, et al: Protein measurement with the Folin phenol reagent. *J Biol Chem* 193:265-275, 1951
10. Newby AC, Luzio JP, Hales CN: The properties and extracellular location of 5'-nucleotidase of the rat fat cell plasma membrane. *Biochem J* 146:625-633, 1975
11. Goll A, Ferry DR, Glossmann H: Target size analysis of skeletal muscle  $\text{Ca}^{++}$  channels: Positive allosteric heterotropic regulation by D-cis-diltiazem is associated with apparent channel oligomer dissociation. *FEBS Lett* 157:63-69, 1983
12. Borgers M, Thone F, Verheyen A, et al: Localization of calcium in skeletal and cardiac muscle. *Histochem J* 16:295-309, 1984
13. Mata M, Staple J, Fink DJ: Ultrastructural distribution of  $\text{Ca}^{++}$  within neurons. *Histochemistry* 87:339-349, 1987
14. Mizuhira V, Notoya M, Hasegawa H: New tissue fixation method for cytochemistry using microwave irradiation. *Acta Histochem Cytochem* 23:501-536, 1990
15. Ellis SB, Williams ME, Ways NR, et al: Sequence and expression of mRNAs encoding the  $\alpha_1$  and  $\alpha_2$  subunits of a DHP-sensitive calcium channel. *Science* 241:1661-1664, 1988
16. Kjeldsen K, Brændgaard H, Sidenius P, et al: Diabetes decreases  $\text{Na}^+\text{-K}^+$  pump concentration in skeletal muscles, heart ventricular muscle, and peripheral nerves of rat. *Diabetes* 36:842-848, 1987
17. Taira Y, Hata T, Ganguly PK, et al: Increased sarcolemmal  $\text{Ca}^{2+}$  transport activity in skeletal muscle of diabetic rats. *Am J Physiol* 260:E626-E632, 1991
18. Chao TT, Ianuzzo CD, Armstrong RB, et al: Ultrastructural alterations in skeletal muscle fibers of streptozocin-diabetic rats. *Cell Tissue Res* 168:239-246, 1976
19. Hayat LH, Crompton N: Evidence for the existence of regulatory sites for  $\text{Ca}^{2+}$  on the  $\text{Na}^+/\text{Ca}^{2+}$  carrier of cardiac mitochondria. *Biochem J* 202:509-518, 1982
20. McCormack JG, Halestrap AP, Denton RM: Role of calcium ions in regulation of mammalian intramitochondrial metabolism. *Physiol Rev* 70:391-425, 1990
21. Ferrari R, Raddino R, Visioli O: The effects of ruthenium red on mitochondrial function during post-ischaemic reperfusion. *J Mol Cell Cardiol* 14:737-740, 1982
22. Crompton M, Costi A, Hayat L: Evidence for the presence of a reversible  $\text{Ca}^{2+}$ -dependent pore activated by oxidative stress in heart mitochondria. *Biochem J* 245:915-918, 1987